© 2022. Published by The Company of Biologists Ltd | Journal of Experimental Biology (2022) 225, jeb243989. doi:10.1242/jeb.243989

RESEARCH ARTICLE

Breathing versus feeding in the Pacific hagfish

Junho Eom[1,2,*,‡], Henrik Lauridsen[3,*] and Chris M. Wood[1,2]

ABSTRACT

Hagfish represent the oldest extant connection to the ancestral vertebrates, but their physiology is not well understood. Using behavioural (video), physiological (respirometry, flow measurements), classical morphological (dissection, silicone injection) and modern imaging approaches (micro-MRI, DICE micro-CT), we examined the interface between feeding and the unique breathing mechanism (nostril opening, high-frequency velum contraction, low-frequency gill pouch contraction and pharyngo-cutaneous duct contraction) in the Pacific hagfish, *Eptatretus stoutii*. A video tour via micro-MRI is presented through the breathing and feeding passages. We have reconciled an earlier disagreement as to the position of the velum chamber, which powers inhalation through the nostril, placing it downstream of the merging point of the food and water passage, such that the oronasal septum terminates at the anterior end of the velum chamber. When feeding occurs by engulfment of large chunks by the dental plates, food movement through the chamber may transiently interfere with breathing. Swallowing is accelerated by peristaltic body undulation involving the ventral musculature, and is complete within 5 s. After a large meal (anchovy, 20% body mass), hagfish remain motionless, defaecating bones and scales at 1.7 days and an intestinal peritrophic membrane at 5 days. O_2 consumption rate approximately doubles within 1 h of feeding, remaining elevated for 12–24 h. This is achieved by combinations of elevated O_2 utilization and ventilatory flow, the latter caused by varying increases in velar contraction frequency and stroke volume. Additional imaging casts light on the reasons for the trend for greater O_2 utilization by more posterior pouches and the pharyngo-cutaneous duct in fasted hagfish.

KEY WORDS: DICE micro-CT, Engulfment, Gill pouches, Oxygen consumption rate, $\dot{M}_{O_2}$, Micro-MRI, Ventilation

INTRODUCTION

Hagfish (Phylum Agnatha) may be the oldest extant representatives of the most ancient vertebrate lineage, though this remains controversial (Bardack, 1998; Oisi et al., 2013; Miyashita, 2020). Certainly, they are very different from modern fishes, and of key importance in phylogenetic debates with respect to anatomical, physiological and molecular aspects of early vertebrate evolution. Sadly, they are also endangered by a targeted, rapidly expanding and unsustainable world-wide fishery; 10% of known species are now red-listed by the International Union for the Conservation of Nature, and another 40% are classified as data deficient (Ellis et al., 2015). Hagfish are difficult to study in captivity, for multiple reasons elaborated by Glover et al. (2019), and many aspects of their biology remain unknown. There is a critical need to learn more about the basic physiology of this evolutionarily significant group.

What little is known about their respiratory physiology has been summarized by Johansen and Strahan (1963), Bartels (1988) and Malte and Lomholt (1988). Their breathing mechanism is unique amongst fish. Water is inspired exclusively via a single central nostril; there appears to be no water entry through the mouth. In the Pacific hagfish *Eptatretus stoutii*, Eom and Wood (2019) described a two-phase pumping system in which ventilatory flow is powered by rhythmic contraction of a single velum chamber that creates suction for inhalation via the nostril, then forces the water down a very long pharynx leading to 24 separate gill pouches (12 per side) as well as into the common pharyngo-cutaneous duct (PCD). The PCD is an apparent bypass shunting system with a separate exit on the left side. The gill pouches and PCD contract at a much lower rate than the velum chamber, and these contractions help drive exhalation through the 24 separate efferent branchial ducts and the PCD aperture. There are gill lamellae in each pouch (but not in the PCD) and the direction of water flow is thought to be countercurrent to the direction of blood flow (Mallatt and Paulsen, 1986). There are no data on ventilation or O_2 extraction at the gills in fed hagfish. However, in fasting hagfish, resting oxygen consumption rate ($\dot{M}_{O_2}$) and O_2 utilization at the gills are low relative to those of other fish (Eom and Wood, 2021). There is also a gradient in O_2 extraction, with the highest expired O_2 partial pressure (P_{O_2}) values at the exits of the anterior gill pouches (i.e. least O_2 utilization), and lowest expired P_{O_2} values at the exits of the most posterior gill pouches and PCD (i.e. greatest O_2 utilization) (Eom and Wood, 2021). When ventilatory flow spontaneously increases above resting levels, $\dot{M}_{O_2}$ increases in parallel. Increases in ventilatory flow can be achieved by increases in either ventilatory stroke volume or velar contraction frequency (hereafter velar frequency), or both (Eom and Wood, 2019; Eom et al., 2019), but O_2 extraction efficiency (utilization) remains fairly constant (Eom and Wood, 2021).

There is only sparse information on the feeding physiology of hagfish, and its metabolic consequences (reviewed by Martini, 1998; Glover and Bucking, 2015; Glover and Weinrauch, 2019). Indeed, in a recent Commentary in *Journal of Experimental Biology*, Glover and Weinrauch (2019) highlighted the need for more studies on this aspect of their physiology. Hagfish are traditionally known as scavengers on dead and dying vertebrates, burrowing into the carcasses (Shelton, 1978; Martini, 1998), and some nutrients may be directly absorbed through the skin (Glover et al., 2011). Less widely appreciated is the fact that hagfish are also active predators. Zintzen et al. (2011) documented targeted predation on fish buried in sand at depth in the wild. Hagfish are virtually blind, but find their prey by olfactory cues (Tamburri and Barry, 1999; Glover et al., 2019), probably detected by densely packed chemosensory cells (Schreiner organs;

[1]Department of Zoology, University of British Columbia, Vancouver, BC, Canada V6T 1Z4. [2]Bamfield Marine Sciences Centre, Bamfield, BC, Canada V0R 1B0. [3]Department of Clinical Medicine, Aarhus University, DK-8200 Aarhus N, Denmark.
*These two authors contributed equally to this paper and are joint first authors

‡Author for correspondence (june@zoology.ubc.ca)

J.E., 0000-0003-0278-0082; H.L., 0000-0002-8833-4456; C.M.W., 0000-0002-9542-2219

Received 8 January 2022; Accepted 24 February 2022

Journal of Experimental Biology (2022) 225, jeb243989. doi:10.1242/jeb.243989

Braun and Northcutt, 1998) in the anterior body surface together with olfactory rosettes (Theisen, 1973). Although lacking jaws, hagfish are very capable of grasping prey with their dental plates and teeth, which can be advanced on either side of the mouth (Clark and Summers, 2007; Clark et al., 2010), followed by ingestion through the mouth apparatus – feeding by 'engulfment' (Eom and Wood, 2019). Various cartilaginous structures and complex deep protractor, clavatus, perpendicularis and tubulatus muscles are involved, enabling the dental plates and keratinous teeth to move forwards and backwards for grasping and pulling the prey objects. Several contraction cycles may be needed to force the food down the tract (Clark and Summers, 2007). Subsequent digestion and absorption appear to be slow processes, with morphological changes in the gut and long-lasting but variable post-prandial elevations (8–72 h) in ammonia excretion and O_2 consumption ($\dot{M}_{O_2}$) (Wilkie et al., 2017; Weinrauch et al., 2018; Glover et al., 2019). However, these two studies did not examine feeding by engulfment, but rather used either force feeding of low ration (5% of body mass) by gavage (Glover et al., 2019) or voluntary feeding of unknown ration by allowing the animals to bury into the carcass of a dead hake (Weinrauch et al., 2018).

In the present study, we employed behavioural, physiological and morphological approaches to investigate the interface of feeding versus breathing in *Eptatretus stoutii*. Our particular focus was on voluntary feeding by engulfment, which ensures consumption of a high ration (~20% of body mass), on the structures and pathways involved, and on the respiratory consequences. Clearly, there would be a potential for large chunks of ingested prey to interfere with the rhythmic pumping of the velum chamber. We employed both classical morphological approaches (dissection, silicone injection, video recording) and state of the art imaging techniques: diffusible iodine-based contrast-enhanced micro-computed tomography (DICE micro-CT) and high field micro-magnetic resonance imaging (micro-MRI). The latter was used to construct a visual tour through the breathing and feeding passages of the hagfish head. Previous anatomical uncertainties were resolved. We videoed the natural engulfment feeding behaviour in the laboratory, recorded the swallowing action, and then followed the hagfish to see how long it took to complete digestion. As the two previous reports of $\dot{M}_{O_2}$ elevation after feeding differ in both methodology and observed responses (Weinrauch et al., 2018; Glover et al., 2019), we characterized patterns for 24 h after feeding by engulfment. In addition to $\dot{M}_{O_2}$, we also examined whether ventilatory flow (the product of velar frequency and stroke volume), branchial O_2 utilization or both increased, and whether the anterior-to-posterior gradient in O_2 utilization persisted. Eom and Wood (2021) suggested several possible explanations for this gradient, including rebreathing of water from one pouch to the next as it passed posteriorly prior to expulsion. Our objective was to see whether there was any morphological basis for such re-breathing.

Based on the prior information summarized above, our specific hypotheses were: (i) that there would be anatomical separation of feeding versus breathing passages, such that rhythmic velum chamber contraction would not be blocked by engulfed prey objects; (ii) that there would be a morphological basis for the gradient in O_2 utilization from the anterior to posterior gill pouches seen in resting fasted hagfish; (iii) that the expected $\dot{M}_{O_2}$ elevation after feeding would be accompanied by increases in ventilatory flow as a result of elevations in both stroke volume and velar frequency, but little change in O_2 utilization; and (iv) that the high ration associated with engulfment feeding would result in more marked elevation of $\dot{M}_{O_2}$ than reported in previous studies (Weinrauch et al., 2018; Glover et al., 2019).

MATERIALS AND METHODS

Experimental animals

Pacific hagfish, *Eptatretus stoutii* (Lockington 1878) (average body mass 99.1 g, range 71.8–158.3 g) were collected in Trevor channel (48° 50.844′ N, 125° 08.321′ W, depth 100 m) on the west coast of Vancouver Island, BC, Canada under permits (XR 194 2017, XR 204 2018, XR 212 2019, XR 136 2021) from the Department of Fisheries and Oceans Canada, using bottom-dwelling traps baited with strips of Pacific hake (*Merluccius productus*). The captured hagfish were transferred to Bamfield Marine Sciences Centre (BMSC) and placed in fibreglass tanks served with flowing seawater (temperature 11–13°C, salinity 30–31 ppt) and several PVC pipes for hiding shelters. The hagfish were fasted over 2–3 weeks and fed only during experiments. Prior to experiments, the hagfish were weighed. Most experiments were performed during the hours of darkness, starting in the early evening, and the animals were shielded from direct light. After experiments, the hagfish were euthanized using an overdose of tricaine methane sulfonate (MS-222, 5 g l^{-1} neutralized to pH 7.8 with 5 mol l^{-1} NaOH; Syndel laboratories, Parksville, BC, Canada) and then eviscerated to ensure death. The experiments reported here were performed under animal usage permits (AUP) approved by the University of British Columbia (UBC, A14-0251, A18-0271) and BMSC Animal Care Committees (AUP RS-17-20, RS-18-20, RS-19-20-21-15), and followed the guidelines of the Canadian Council of Animal Care.

Nostril operation for measuring ventilation flow in fasted and fed hagfish

The hagfish generates unidirectional ventilation, inhaling water through a single central nostril duct and exhaling it to the ambient environment through ~12 pairs of gill pouches and the PCD. The flow is generated by high-frequency velum movement, with low-frequency gill pouch and PCD contraction aiding exhalation (Eom and Wood, 2019; Eom and Wood, 2021). Direct measurement of total ventilatory flow is only possible by placing a flow probe on a tube implanted in the nostril (Perry et al., 2009; Eom and Wood, 2019). However, hagfish cannot feed when the nostril tube is in place. Therefore, in order to monitor ventilation immediately after feeding, hagfish were allowed to feed normally as described below, and then, within 1 min, an operation was initiated to install the nostril tube. The hagfish were quickly anaesthetized in MS-222 (0.6 g l^{-1}, neutralized to pH 7.8 with 5 mol l^{-1} NaOH) for 1–2 min. Hagfish are known to be hypoxia tolerant, so the anaesthetized hagfish were placed on an operating table without gill irrigation, and their bodies were moistened with wet tissue. A 3 cm length of transparent silicone tubing (6.35 mm o.d. and 4.32 mm i.d.) was inserted into the nostril duct and sutured by two stitches (26 mm 1/2C taper, Perma-Hand Silk, Ethicon, Somerville, NJ, USA) to the skin around the nostril opening area. After the operation, each hagfish was placed in a plastic container (20 cm×20 cm×15 cm) served with flowing seawater. The hagfish resumed their normal coiled posture within 5 min.

An ultrasonic microcirculation blood flow probe (V-series, Transonic Systems Inc., Ithaca, NY, USA) connected to a flow meter (T206, Transonic Systems Inc.) was gently connected to the silicone nostril tube of the recovered hagfish with minimal disturbance, and the total ventilatory flow rate was measured. The measured ventilation signal was converted into digital signals in a

PowerLab data integrity system (ADInstruments, Colorado Springs, CO, USA), and visualized in LabChart software v. 7.0 (ADInstruments). Using analysis functions in LabChart, the ventilation flow ($\dot{V}_w$, ml min^{-1}) and frequency (f_R, min^{-1}) were analysed and averaged per 30 s intervals. The averaged ventilation flow data were divided by fish body mass in order to yield mass-specific $\dot{V}_w$ (ml kg^{-1} min^{-1}). Then, the standardized $\dot{V}_w$ was divided by the measured frequency (f_R) so the mean stroke volume (SV_w, ml kg^{-1}) was calculated. During ventilation measurement, artifacts such as electrical and physical non-specific noise signals were also detected, especially between 1 and 10 Hz, so they were automatically removed by a low-pass filter in LabChart. It was essential to set the correct orientation of the flow probe as it detects the direction of flow during experiments. Two-point system calibration was checked in the flow meter (Transonic Systems Inc.), and also extrinsic calibration was performed by flowing BMSC seawater (12°C, 31 ppt) through the flow probe at known rates using an aqua lifter vacuum pump (Cheng Gao Plastic and Hardware Electricity, Dongguan, Guangdong, China).

Series I: observation of voluntary feeding behaviour in the laboratory environment

Prior to the experiment, frozen anchovies (*Engraulis mordax*) were completely thawed in seawater. Two or more hagfish were placed in a round glass bowl filled with 5 l of seawater. Within 5 min, the hagfish exhibited a coiled posture and stayed at the bottom of the glass bowl. Four or five thawed chunks of anchovies (~10 g per chunk) were then placed into the glass bowl. In order to stimulate feeding behaviour, 3–5 ml of anchovy juice extracted from decayed anchovy chunks incubated in seawater at room temperature was also added. In order to record the overall feeding event, the glass bowl was elevated to a height of 60 cm, so as to facilitate video recording by a portable industrial camera (USB 2 µEye ME, IDS Imaging Development Systems GmbH, Obersulm, Germany) mounted underneath the glass bowl. Review of the video recordings confirmed the amount consumed by each hagfish. In some trials, each anchovy chunk contained a small magnet (<1 g), so the engulfed anchovy chunk could be detected externally by a magnetic detector (AMY6, General Tools Secaucus, NJ, USA). After completion of feeding behaviour, the hagfish resumed their coiled posture and did not show further attraction to the remaining anchovy chunks. In some trials, the fed hagfish were moved to individual plastic containers served with flowing seawater and monitored at least 10 times per day for up to 5 days. In some of these fed hagfish, their responsiveness was tested by gentle pinching or transfer to another container, procedures which invariably elicit activity in fasted hagfish. In other trials, the fed hagfish were then immediately used for whole-animal respirometry (series II), nostril operation (series III), and/or P_{O_2} recording (series IV). In all tests, in order to minimize stress, which could result in slime generation, we moved the hagfish using a fine net instead of bare hands.

Series II: measurement of $\dot{M}_{O_2}$ by respirometry in voluntarily fed hagfish

Experiments were started in the evening (19:00–21:00 h). Hagfish (N=8) were allowed to feed voluntarily on pre-weighed chunks of anchovy as described above, and the amount of food ingested was recorded. We watched the individual hagfish, identified by slightly different sizes, throughout the feeding period, so we could quantify how much food in total was eaten by each one. The animals were then placed individually in 1 l darkened glass jars served with flowing seawater, and standing in a running seawater bath to maintain 12°C. Periodically, flow was stopped, the jars were sealed, and the decline in P_{O_2} over approximately 30 min (exact time noted) was recorded using a galvanic oxygen electrode and meter (DO 6+, Oakton Instruments, Vernon Hills, IL, USA), so as to measure $\dot{M}_{O_2}$ at 0.5, 1, 2, 4, 8, 12, 18 and 24 h after feeding. A parallel control group of hagfish were put through an identical procedure, including exposure to anchovy juice to initiate excitement, but were not allowed to feed, followed by $\dot{M}_{O_2}$ measurements at the same times. Blank measurements demonstrated no significant decline in P_{O_2} over 30 min.

$\dot{M}_{O_2}$ (µmol kg^{-1} h^{-1}) was calculated as:

$$\dot{M}_{O_2} = \Delta P_{O_2} \times \alpha_{O_2} \times V \times M^{-1} \times t^{-1}, \quad (1)$$

where ΔP_{O_2} is the decline in water P_{O_2} (Torr), α_{O_2} is the appropriate oxygen solubility coefficient (1.7747 µmol Torr^{-1} l^{-1}) for 31 ppt sea water at 12°C (Boutilier et al., 1984), V is volume (l) of water, M is body mass (kg) of the hagfish and t is time (h).

Series III: measurement of respiration and nostril ventilation in voluntarily fed hagfish

After feeding (again at 19:00–21:00 h) and nostril operation as described above, ventilatory flow ($\dot{V}_w$) recordings were started by attaching the flow probe to the nostril tube as soon as the hagfish resumed its resting coiled posture (~5 min). The flow probe was left in place for periods of up to 60 min for recordings at 1, 4 and 24 h after feeding (N=6–7 at each time). We found that if the flow probe was left attached in the intervening periods, the hagfish became restless. Data for fasted controls were compiled from measurements in non-fed control animals (N=40). In these control experiments, the hagfish were completely resting and had not been subjected to exposure to anchovy juice to initiate excitement. The measured $\dot{V}_w$, and inspired and expired P_{O_2} ($P_{I_{O_2}}$ and $P_{E_{O_2}}$) were used for calculating the $\dot{M}_{O_2}$ (Eqn 3), as in series IV.

Series IV: measurement of P_{O_2} from 12 gill openings and the PCD

Individual hagfish were placed in a 2 l plastic container served with flowing seawater, and P_{O_2} recordings were made within 0–1 h of feeding, and again at 4 and 24 h after feeding (N=6–8 at each time). As in series III, data for fasted controls were compiled from measurements in non-fed resting animals (N=16) that had not been subjected to exposure to anchovy juice to initiate excitement. To make measurements, we gently flipped over the coiled hagfish to expose the openings of the 12 paired gill pouches and PCD. Although inverted, hagfish still maintained the coiled, resting posture. An O_2 micro-optode probe which was connected to a micro-fibre optic oxygen meter (PreSens, Microx TX3, Precision Sensing GmbH, Regensburg, Germany) was applied within 5 mm of each respective gill opening on one side so as to measure expired water $P_{E_{O_2}}$. The micro-optode was similarly applied to measure $P_{E_{O_2}}$ at the outflow of the PCD. A three-axis micro-manipulator (Narishige, Tokyo, Japan), mounted by magnet on an iron plate placed underneath the plastic container, was used to manoeuvre the micro-optode probe so that the probe position could be finely adjusted during experiments. The order of measurement of the different openings was randomized. Similar to our previous report (Eom and Wood, 2021), the measured $P_{E_{O_2}}$ showed very small rhythmic fluctuations over time. Their rhythmic frequency was much slower than velar movements, and co-ordinated with faint gill pouch contractions. The inhaled water oxygen partial pressure ($P_{I_{O_2}}$)

was also measured at the entrance of the silicone tubing in the fish nostril.

The measured P_{O_2} values were visualized in PowerLab (ADInstruments), analysed in LabChart (ADInstruments), and eventually exported to Excel for further calculation of percentage O_2 utilization from percentage $P_{I_{O_2}}$ and $P_{E_{O_2}}$:

$$O_2 \text{utilization} = (P_{I_{O_2}} - P_{E_{O_2}})/P_{I_{O_2}} \times 100 \quad (2)$$

and $\dot{M}_{O_2}$ (μmol kg^{-1} h^{-1}) by the Fick equation:

$$\dot{M}_{O_2} = (P_{I_{O_2}} - P_{E_{O_2}}) \times \alpha_{O_2} \times \dot{V}_w \times 60 \text{ min h}^{-1}, \quad (3)$$

where $P_{I_{O_2}}$ and $P_{E_{O_2}}$ are in Torr, α_{O_2} is the appropriate oxygen solubility coefficient in μmol Torr^{-1} l^{-1}, and $\dot{V}_w$ is mass-specific ventilatory flow (l kg^{-1} min^{-1}). As inhaled water from the nostril is exhaled through 12 pairs of gill pouches and the PCD, flow rate could not be measured at each gill pouch and may vary among pouches. Therefore, as in Eom and Wood (2021), to calculate $\dot{M}_{O_2}$, we averaged $P_{E_{O_2}}$ values from each gill pouch and the PCD, and applied Eqn 3.

Series V: anatomical studies in hagfish

To image the internal anatomy of the Pacific hagfish, four specimens were used in total for high-field micro-MRI (n=1) and DICE micro-CT (n=4; one of these was the same specimen used for micro-MRI). The hagfish were euthanized as detailed above. Before micro-MRI, the 5 cm cranial portion of the specimen was excised from the remaining body and placed in a 50 ml Falcon™ tube and immersed in Fomblin Y, a H^+ devoid medium providing a completely dark background in H^+-MRI, under a low vacuum to extract air bubbles. MRI was performed on an Agilent 9.4T system equipped with a Rapid-40-H^+ body coil and using a 3D gradient echo sequence with the following parameters: repetition time 19 ms, echo time 3.848 ms, flip angle 30 deg, field of view 50×50×50 mm^3, spatial resolution 0.0977 mm isotropic, number of averages 44, total acquisition time 45 h. Before DICE micro-CT, the samples were stained in Lugol's solution (8.3 g l^{-1} I_2 and 16.6 g l^{-1} KI) for 1–2 weeks (depending on specimen size) with rocking. The cranial portion of the same specimen used for micro-MRI was also used for DICE micro-CT along with the cranial portion of another specimen. Two additional specimens were used to scan the gill pouch portion. Micro-CT was performed using a Scanco Medical XtremeCT system with the following parameters: x-ray tube voltage 59.4 kVp, x-ray tube current 119 μA, 1000 projections per 180 deg, integration time 132 ms, field of view 70×70×70 mm^3, spatial resolution 0.041 mm.

We also performed dissection of freshly euthanized hagfish for which injection of coloured silicone into the nostril duct (red) and the mouth cavity (green or yellow) had been performed. The coloured silicone was prepared by adding red or green commercial food dye (Club House, London, ON, Canada) into ∼20 ml of commercial silicone (Advanced Silicone 2, GE). The silicone was well stirred with a wooden stick for 30 s, placed in a 20 ml disposable syringe, and injected into the nostril duct (red) and mouth cavity (green), respectively. After that, the hagfish was decapitated and the silicone-injected head region was fixed in 4% formalin solution for a week, and then used for dissection.

Statistical analyses

All the measured inspired water O_2 ($P_{I_{O_2}}$), expired water O_2 ($P_{E_{O_2}}$), ventilation flow rate ($\dot{V}_w$), frequency of ventilation (f_R), calculated stroke volume (SV_w), O_2 utilization and oxygen consumption rate ($\dot{M}_{O_2}$) parameters are reported as means±s.e.m. with the number of animals (N). Data were transformed when necessary so as to ensure normality and homogeneity of variance. Two-way repeated measures ANOVA with Tukey's *post hoc* test was used to examine overall effects of feeding, time and their interaction in series II. One-way ANOVA followed by Dunnett's *post hoc* test was performed to evaluate whether the changed physiological variables in fed hagfish were significantly different relative to fasted controls in series III and IV. In series IV, in order to assess potential differences in O_2 utilization among the various gill pouches and PCD, two different analyses were performed. In the first, linear regressions were performed of O_2 utilization against gill pouch order, and the significance of the correlation coefficient was assessed. In the second, one-way ANOVA followed by Tukey's *post hoc* tests were carried out to identify specific differences among pouches. All the statistical tests were conducted in GraphPad Prism software v. 6.0 (La Jolla, CA, USA), and the threshold for statistical significance was P<0.05.

RESULTS

Series I: observation of voluntary feeding behaviour in the laboratory environment

Movie 1 is a video of a bout of active feeding by two hagfish. Hagfish seemed more willing to feed when more than one animal was present. Feeding behaviour appeared to be triggered by olfactory cues, because the freshly thawed anchovy chunks were ignored by the hagfish until the extract of rotten anchovy was added. Shortly thereafter, the hagfish became active, exhibiting orientation towards the chunks, and exposing the dental plates. The following is based on detailed observations on N=8 hagfish. Four stages of feeding behaviours were identified: (1) orientation to chemical cues of anchovy chunks (Fig. 1A), (2) searching for and approaching the chunks (Fig. 1B), (3) exposing the dental plates, biting the chunks, and engulfing the bitten-off parts sequentially (Fig. 1C), and (4) vigorously shaking the anterior body (Fig. 1D). After the hagfish exposed the dental plates, the ventral muscle contraction was observed and it lasted until the engulfed chunks were transferred to the intestine, where they were identified by the magnet detector (Fig. 1E,F,K). The swallowing process took only about 5 s. Maximum engulfing capacity appeared to be about 20% of body mass; each hagfish (∼100 g) usually engulfed two chunks (∼10 g per chunk). The fed hagfish did not show any further attraction to the remaining anchovy chunks (Fig. 1E) and rested motionless in a typical coiled posture. At 1.7 days after feeding, the hagfish appeared to have digested the soft tissues, and defaecation of anchovy bony structures and scales through the anus was observed (Fig. 1G). At 5 days, the fish excreted intestinal membranes (Fig. 1H,I,J; N=3) together with bile and appeared to have finished the digestive and absorptive processes.

Series II: measurement of $\dot{M}_{O_2}$ by respirometry in voluntarily fed hagfish

The fed animals voluntarily ingested 19.74±0.67% (N=8) of their body mass in anchovy chunks. The two-way repeated measures ANOVA revealed significant effects of feeding (P=0.0076) and time (P<0.0001) but their interaction was not significant (P=0.4234) over the 24 h experimental period. $\dot{M}_{O_2}$ approximately doubled by 0.5 h after feeding, becoming significantly different from that of the fasted controls at 0.5–4 h and also at 12 h (Fig. 2). Note that in this series, the controls had been exposed to anchovy juice to initiate excitement, so the significantly higher $\dot{M}_{O_2}$ values in the experimental animals were solely due to actual feeding.

Journal of Experimental Biology (2022) 225, jeb243989. doi:10.1242/jeb.243989

Fig. 1. Hagfish feeding behaviours and digestion of prey items. In response to a chunk of anchovy, hagfish showed four stages of feeding behaviours: orientation and opening of the dental plates (A), searching for and approaching the anchovy (B), engulfing the anchovy (C) and vigorously shaking the anterior body (D). As a result of the shaking behaviour, two pieces of engulfed anchovy were immediately moved through the pharynx within 5 s (E,F,K). A magnet was inserted into each chunk of anchovy (E), so that its position (F) could be externally detected by the magnetic detector (K) (green light in E represents south polarity). Within 1.7 days of feeding (41.3 h; G), anchovy soft tissue was completely digested and apparently indigestible body structures (bones, scales) were excreted through the anus. At 5 days (121.9 h; H–J), an intestine membrane was excreted with bile (images from three different hagfish), and the digestive and absorptive processes appeared to be complete. Scale bars: 1 cm. DP, dental plates; MC, muscle contraction; Ma, magnet; AC, anchovy chunk; C, cloaca; M, mouth; PCD, pharyngo-cutaneous duct; IM, intestine membrane; BA, bile acids; GO, gill openings.

Series III: measurement of respiration and nostril ventilation in voluntarily fed hagfish

In comparison to completely resting non-fed control animals, fed hagfish significantly increased all of their ventilatory parameters, O_2 utilization and $\dot{M}_{O_2}$, but with differential contributions at different times (Fig. 3). Thus, increases in velar frequency (f_R; Fig. 3A, one-way ANOVA, P=0.0022) and total ventilatory flow rate ($\dot{V}_w$; Fig. 3B, P=0.0255) were significant at 24 h, whereas

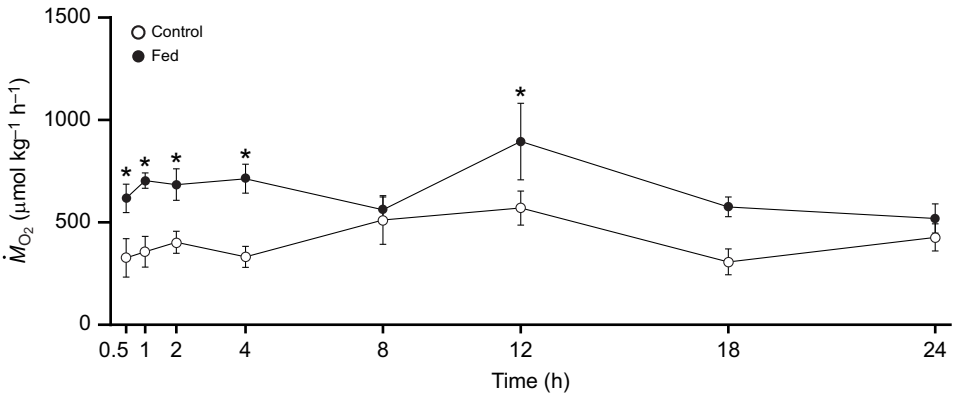

Fig. 2. Oxygen consumption rate ($\dot{M}_{O_2}$) in fasted control and voluntarily fed hagfish over 24 h. Data are means±s.e.m. for control (N=8) and fed (N=8) hagfish. Two-way repeated measures ANOVA demonstrated significant effects of feeding (P=0.0076) and time (P<0.0001) but their interaction was not significant (P=0.4234). Asterisks indicate significantly higher $\dot{M}_{O_2}$ values in fed animals at 0.5–4 h and 12 h post-feeding (Tukey's test) relative to non-fed controls subjected to similar 'pre-feeding' excitement.

Journal of Experimental Biology (2022) 225, jeb243989. doi:10.1242/jeb.243989

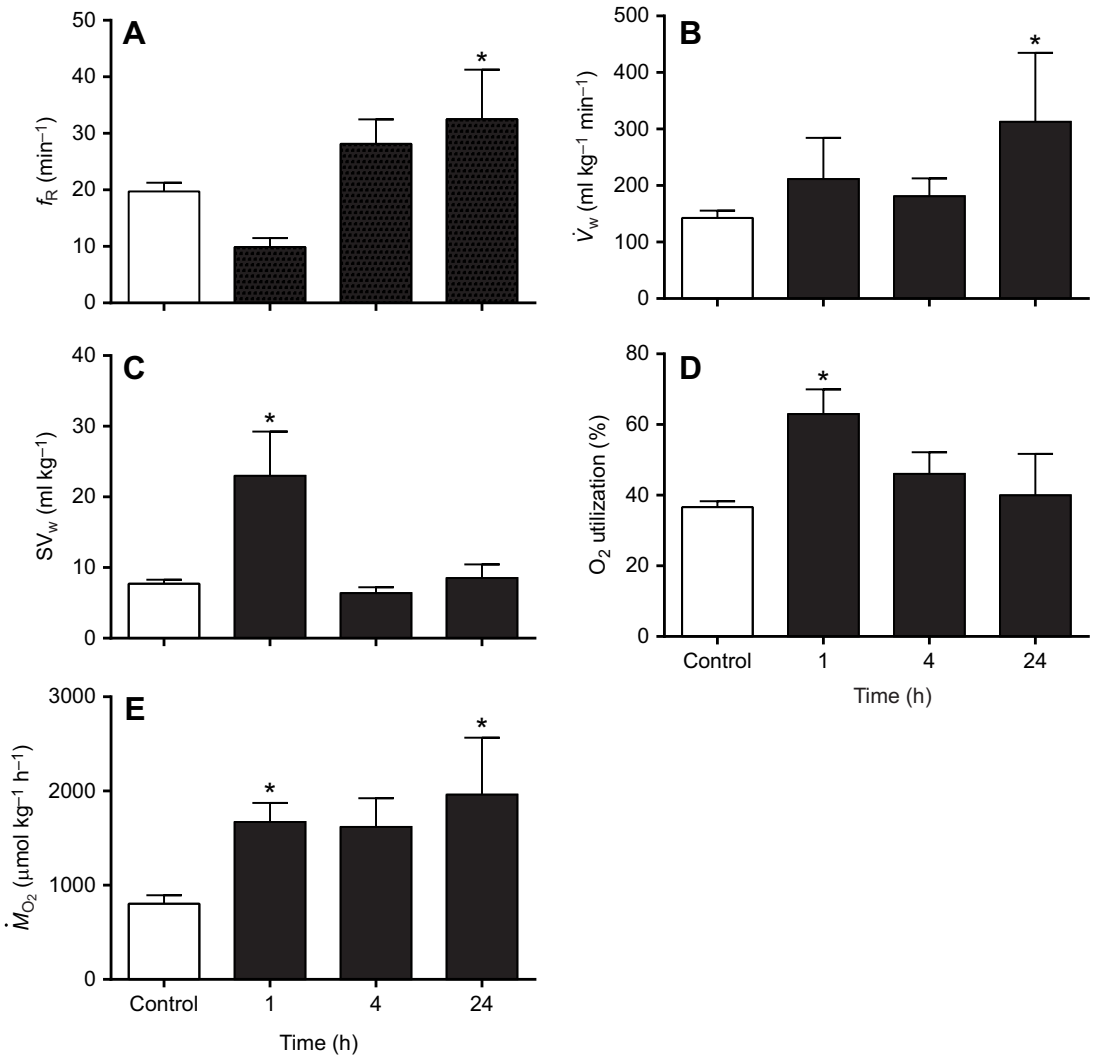

Fig. 3. Hagfish ventilatory parameters, oxygen utilization and $\dot{M}_{O_2}$ after feeding. Compared with fasted controls (N=40), in the first hour, fed hagfish (N=6–7) decreased velar frequency (f_R; A) but increased stroke volume (SV_w; C) (one-way ANOVA, *P<0.0001) and O_2 utilization (D) (*P=0.0028), resulting in increased O_2 consumption ($\dot{M}_{O_2}$; E) (*P=0.0001). At 24 h, the hagfish exhibited significantly increased frequency (A; *P=0.0093) and ventilation flow ($\dot{V}_w$; B) (*P=0.0191), resulting in significantly increased $\dot{M}_{O_2}$ (E; *P=0.0001).

increases in ventilatory stroke volume (SV_w; Fig. 3C, P=0.0013) and mean O_2 utilization (Fig. 3D, P=0.0028) were significant at 1 h, while increases in $\dot{M}_{O_2}$ were significant at both 1 h and 24 h post-feeding (Fig. 3E, P=0.0001). Overall, the increases in $\dot{M}_{O_2}$ relative to controls measured here by the Fick principle were about 2.5-fold, only slightly greater than those measured directly by respirometry in series II (Fig. 2), perhaps reflecting differences in the treatment of the non-fed controls.

Series IV: measurement of P_{O_2} from 12 gill openings and PCD

Measurements of $P_{E_{O_2}}$ during the first hour after feeding demonstrated that the fed hagfish showed almost 2-fold higher O_2 utilization (P=0.0010), averaging ∼66% versus ∼35% in fasting hagfish (Fig. 4). The characteristic trend for progressively increasing O_2 utilization from anterior to posterior pouches and PCD, as previously reported by Eom and Wood (2021), was also seen in the current dataset for fasting fish (Fig. 4A). There was a significant linear correlation (r=0.849, P=0.002) between O_2 utilization and pouch order. One-way ANOVA revealed significant overall variation in utilization among pouches and PCD (P=0.029), though none of the individual differences were significant among the 13 means. However, when the data were combined into three groups (pouches 1–5, pouches 6–12 and PCD) based on the anatomical findings of series V (see below), the one-way ANOVA result was highly significant (P=0.002), with the *post hoc* tests revealing significant differences of pouches 1–5 (lower) versus pouches 6–12 and PCD (higher); pouches 6–12 and PCD were not significantly different. This pattern disappeared in the fed hagfish at 1 h, with no significant differences among the different gill pouch openings, as evaluated by the same analyses (Fig. 4B). As mean utilization gradually decreased at 4 and 24 h after feeding (Fig. 3D), the pattern tended to re-appear but was not significant (data not shown).

Series V: anatomical studies in hagfish

The muscle and cartilage connections were observed in the anterior head region by DICE micro-CT imaging (Fig. 5). The dorsal longitudinal bar is connected to the paired tentacles and ring-shaped cartilage in the nostril duct, while the dental plates are connected to the medio-rostral part of basal plates, in accord with the observations of Oisi et al. (2013).

Journal of Experimental Biology (2022) 225, jeb243989. doi:10.1242/jeb.243989

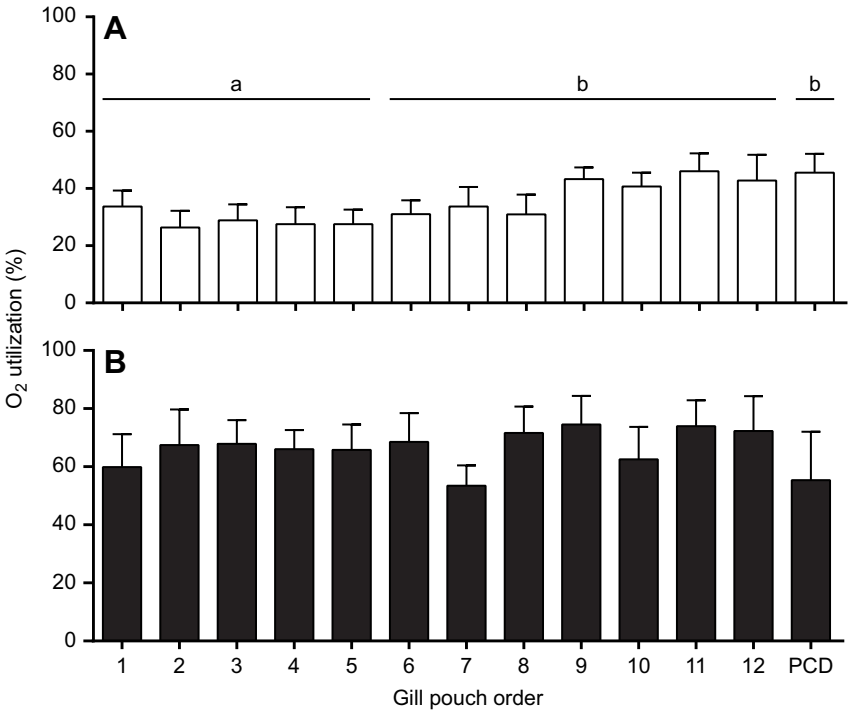

Fig. 4. Oxygen utilization in the gill pouches and PCD in fasted control and voluntarily fed hagfish. (A) Under fasted control conditions, the hagfish (N=16) utilized approximately 35% (35.2±2.0%) of the inspired O_2 on average. There was a significant correlation between O_2 utilization and pouch order (r=0.849, P=0.002), and one-way ANOVA revealed significant variation in utilization among the 12 pouches and the PCD, but none of the individual differences was significant. However, when the data were combined into three groups based on the anatomical findings of series V, the variation was highly significant (P=0.002) with pouches 1–5 exhibiting significantly lower O_2 utilization relative to pouches 6–12 and the PCD, as indicated by different letters. (B) These trends were not seen in the first hour after feeding (N=6), where the fish increased overall O_2 utilization almost 2-fold (P=0.001) to approximately 66% (66.1±1.9%) regardless of the anterior versus posterior position of the gill pouches. There was no significant variation among pouches in these fed hagfish.

During hyperventilation, the hagfish vigorously moved specific areas (white dotted areas in Fig. 6A) located 1–2 cm posterior from the eye spot, indicating the position of the velum chamber, which is the fast-suction pump used for inhalation in the hagfish (Eom and Wood, 2019). This movement can be clearly seen in Movie 2. The location of the velum chamber was matched to other anatomical images between lines 4 and 5 in Fig. 6B–F. Fig. 6B is an MRI image showing a mid-sagittal view of the hagfish head. Note that the oronasal septum divides the nostril duct from the mouth cavity, and ends at line 4. Fig. 5C is a lateral view of the hagfish head in micro-MRI; internal bony and cartilaginous structures were sagittally (Fig. 6D) and dorsally (Fig. 6E) visualized in micro-MRI images. Note the presence of four pairs of cartilaginous or bony structures (between lines 4 and 5) that likely form parts of the velum apparatus. Note also the paired dental plates attached to the protractor muscle (between lines 1 and 3). Fig. 6F,G shows photographs of mid-sagittal views of the dissected hagfish head, which had been injected through the nasal duct with red silicone and through the mouth cavity with yellow (Fig. 6F) or green (Fig. 6G) silicone. Note that the yellow silicone injected through the mouth cavity started to merge with the red silicone in a particular area (Fig. 6F); this area was visualized after removing the silicone and matched to the position of the velum chamber (Fig. 6G). A schematic diagram of the mid-sagittal view of the hagfish head was prepared using the information from the above panels (Fig. 6H). The dental plates and the various bony and cartilaginous structures of the velum chamber were outlined from Fig. 6D and recreated in Fig. 6H.

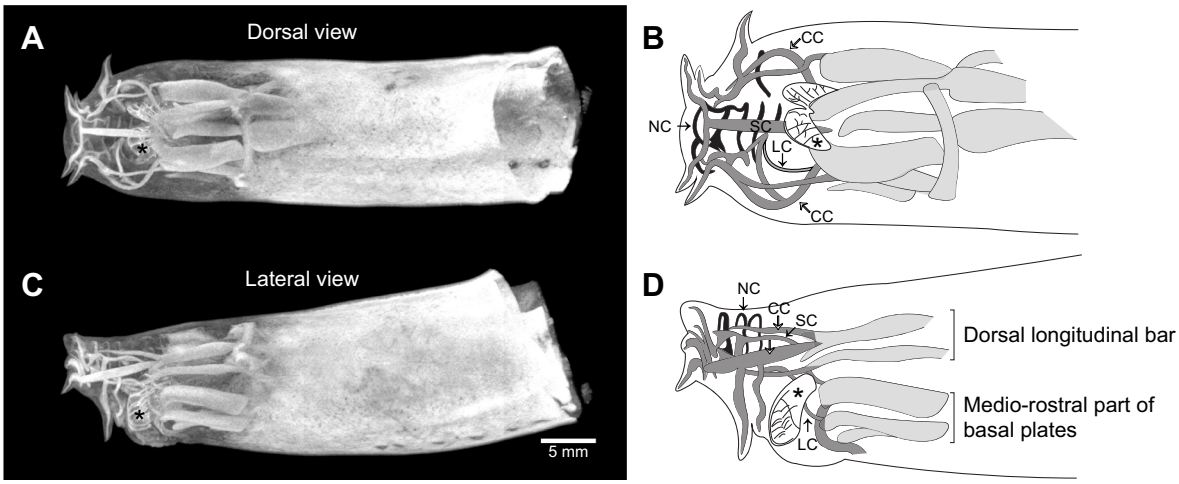

Fig. 5. Images of the hagfish anterior body. (A,C) Computed tomography (CT) images of the anterior hagfish body. (B,D) Corresponding labelled outlines of the images. Paired tentacles are connected to the dorsal longitudinal bar while dental plates (asterisks) are connected to the medio-rostral part of basal plates. Nasal duct cartilage (NC, black) is clearly observed. Overall anatomical structures were identified using the description of Oisi et al. (2013). CC, cornual cartilage; LC, labial cartilage; SC, subnasal cartilage.

Journal of Experimental Biology (2022) 225, jeb243989. doi:10.1242/jeb.243989

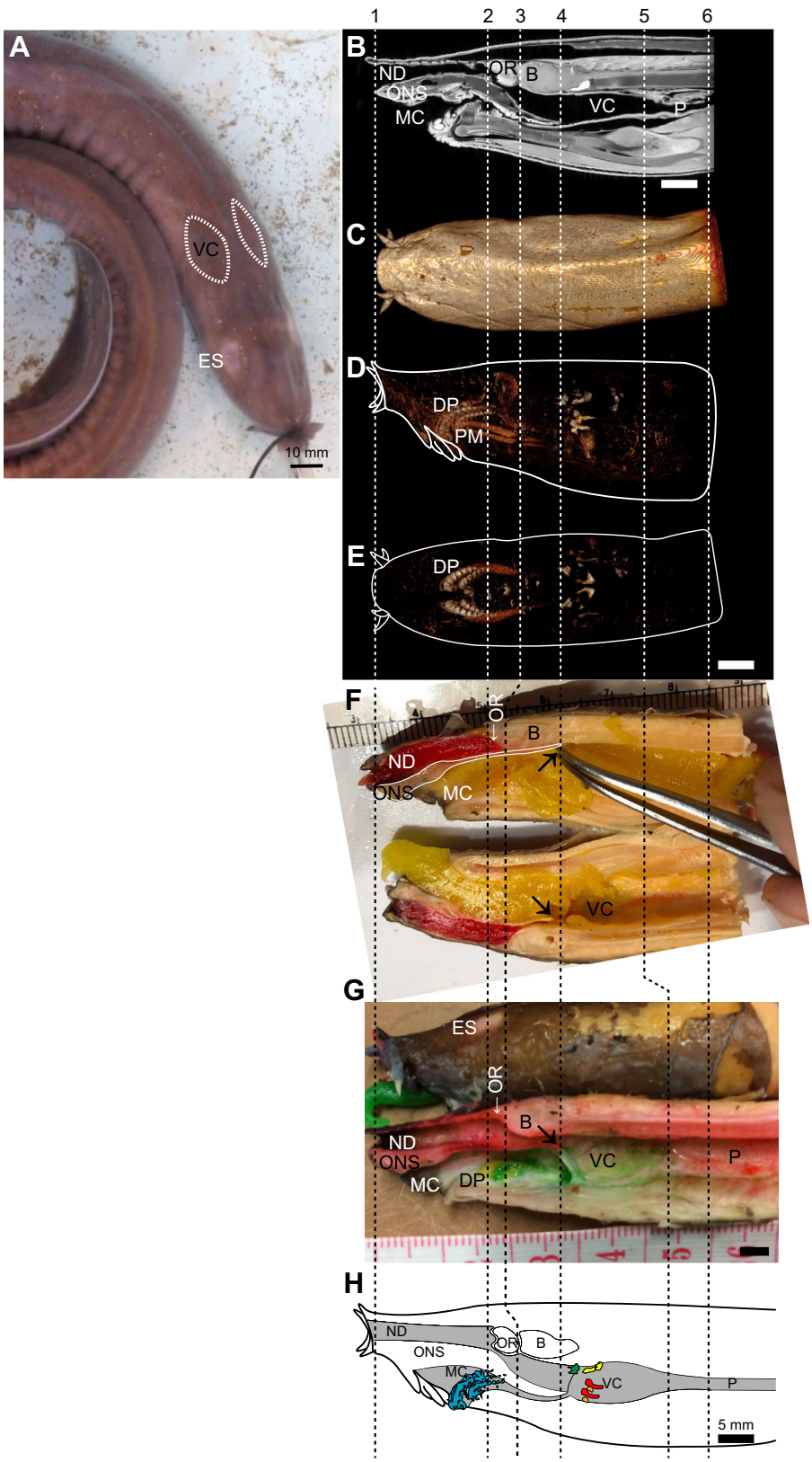

Fig. 6. Anatomy of the head region of the hagfish. (A) Video recording, (B) MRI and (C–E) micro-MRI analysis of the hagfish head, compared with dissected hagfish specimens infused with coloured silicone (F,G). (H) Schematic diagram of the hagfish head region. In the video recording of the hyperventilating hagfish (see Movie 2), symmetrical areas (A, dashed areas) that were located 1–2 cm posterior to the eye spot (ES) were actively moving, indicating the likely position of the velum chamber (VC). The velum chamber was then located between lines 4 and 5 in B–F, and connected to the nostril duct (ND) and mouth cavity (MC) in the MRI image (B). Also, the potential velum chamber area was wrapped with four pairs of cartilage and other bony or cartilaginous structures in micro-MRI images (D,E); these cartilage pairs would support the chamber-like structure (the VC) (G). In F and G, red silicone injected via the nostril duct merged with yellow (F) or green silicone (G) injected via the mouth cavity at the apparent position of the velum chamber. The schematic diagram in H was designed using the MRI image in B by adding paired cartilage in the velum chamber area and dental plates (DP) as detected in D. Scale bar in A: 10 mm; scale bars in B–H: 5 mm. B, brain; ONS, oronasal septum; OR, olfactory rosette; P, pharynx; PM, protractor muscle.

Movie 3 is a video of a micro-MRI tour through the breathing and feeding passages of the anterior part of the hagfish head. We enter anteriorly through the nostril, move under the olfactory rosettes to the potential velum chamber area, and then turn around 180 deg, re-enter, and exit to the environment through the mouth cavity. At the start, we are viewing the hagfish's head from the anterior; note the nostril surrounded by paired tentacles with the mouth opening visible in the midline below the nostril. The dental plates are retracted and are not visible. At 14 s, we enter the nostril and reach the start of the olfactory rosettes, which can be seen on the dorsal surface at 25 s. At 40 s, we reach a small wrinkled chamber which ventrally lies over and is linked to the oronasal septum, leading to a

Journal of Experimental Biology (2022) 225, jeb243989. doi:10.1242/jeb.243989

large chamber-like area, likely the start of the velum chamber. At 55 s, we enter into the potential velum chamber and at 60 s we turn direction by 180 deg. After entering the underside of the wrinkled small chamber which is matched to the posterior end of the oronasal septum at 80 s, we reach the mouth cavity and exit to the environment at 110 s.

Connections from the gill pouches to respiratory and vascular tracts were observed by means of DICE micro-CT (Fig. 7A–C) and

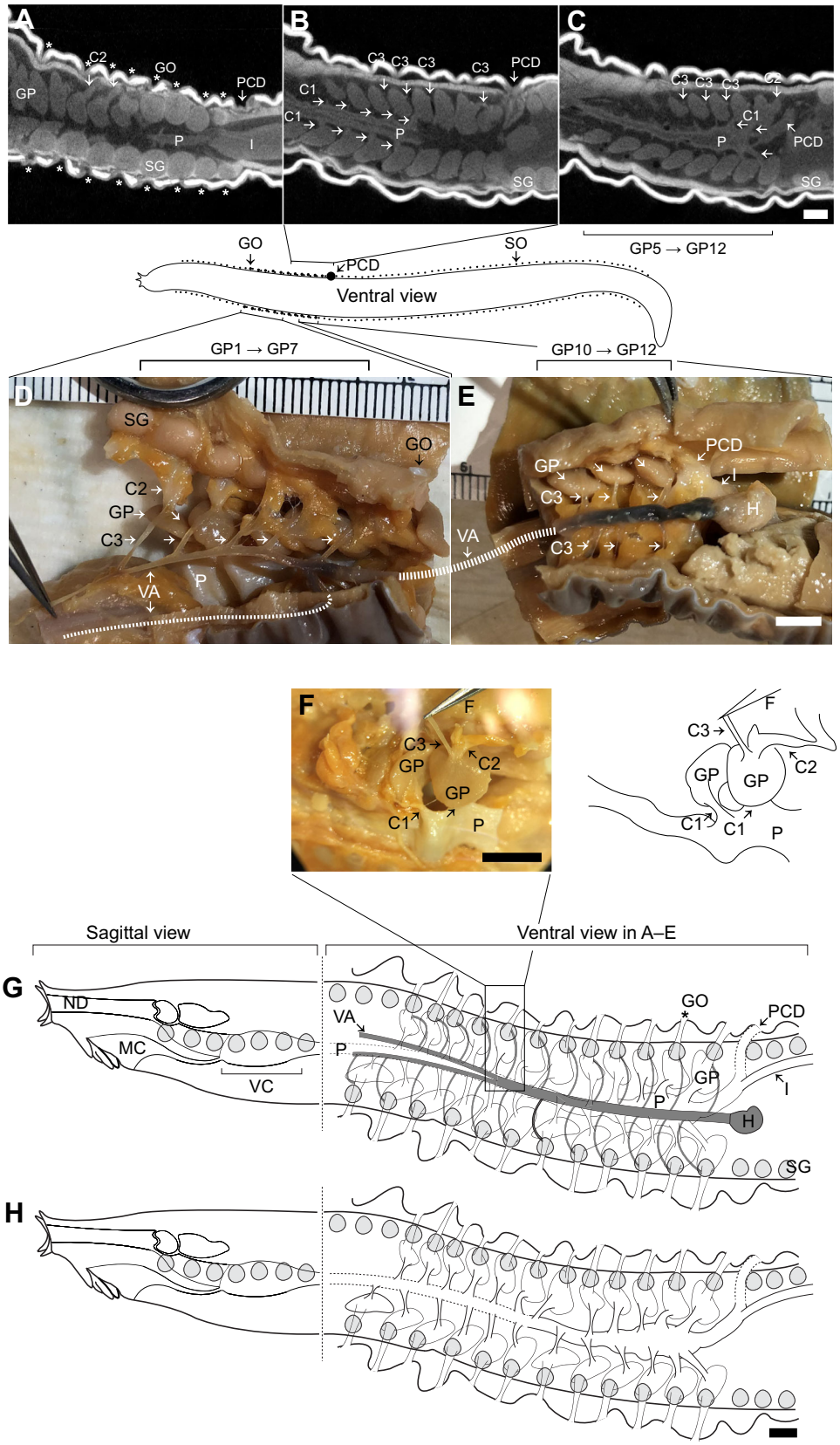

Fig. 7. Analysis of connections from the gill pouches to respiratory and vascular tracts. (A–C) DICE micro-CT analysis and (D–F) dissections of hagfish gill pouches from dorsal to ventral. In A–G, three connections were verified in the gill pouches, including the pharyngo-cutaneous duct (PCD): connection 1 (C1) from pharynx (P) to gill pouch (GP), connection 2 (C2) from gill pouch to gill opening (GO), and connection 3 (C3) from ventral aorta (VA) to gill pouch. (H) All gill pouches including the PCD and the intestine are indirectly connected through the pharynx. In G, C3 connects to the heart (H) via the ventral aorta (VA); the C3 connections of the anterior gill pouches are to the bifurcated ventral aorta while the posterior ones are to the single median ventral aorta. Scale bars: 5 mm. F, forceps; I, intestine; ML, muscle layer; SL, skin layer; SO, slime opening; SG, slime gland.

Journal of Experimental Biology (2022) 225, jeb243989. doi:10.1242/jeb.243989

dissections (Fig. 7D–F). Each gill pouch possessed three visualized connections: pharynx to gill pouch representing connection 1 (C1) and gill pouch to gill opening representing C2 in the respiratory tract, and ventral aorta to gill pouch representing C3 in the vascular tract. Based on the DICE micro-CT imaging, we initially (mis)interpreted the structures marked 'C3' in Fig. 7B,C as functional connections for water flow between adjacent gill pouches. However, careful dissection of preserved material could not confirm their presence. We then realized that these were the afferent branches from the ventral aorta to the gill pouches passing into the plane of sectioning of the DICE micro-CT. In the vascular tract, C3 in the anterior gill pouches between gill pouch 1 and gill pouch 5 goes to the separate branches of the bifurcated ventral aorta, but the remainder of the C3 connections in the posterior gill pouches are to the single median ventral aorta, which in turn arises from the heart. As a result of C1 connections, all gill pouches including the PCD are indirectly connected via the pharynx to the intestine.

DISCUSSION

In the Pacific hagfish, a representative of the oldest extant connection to the ancestral vertebrates, the pharynx is a part of the respiratory tract and connects to the intestine. It is used for both breathing and feeding. As the pharynx serves dual purposes, the rhythmic movement of breathing could be impeded by engulfment of large prey chunks during feeding or vice versa. In this study, therefore, we documented that feeding by engulfment occurs in *E. stoutii* and tried to understand how the hagfish coordinated breathing with the engulfment and swallowing processes, using visual observation together with physiological measurements and anatomical studies of the anterior hagfish body including the respiratory tract. Our study also looked at the behavioural and physiological aspects of feeding and respiration.

The location of the velum chamber

Our first hypothesis, that there would be anatomical separation of feeding versus breathing passages, was not supported. To provide some background, most published models (e.g. Strahan, 1958; Johansen and Strahan, 1963; Li and Wang, 2021) are based on the Atlantic hagfish (*Myxine glutinosa*) and portray the feeding pathway (mouth) and breathing pathway (nostril duct) uniting anterior to the velum chamber. This would not be a problem when the ingested food is a slurry obtained by rasping. However, in the Pacific hagfish (*E. stoutii*), which can feed by engulfment of large chunks of prey, Eom and Wood (2019) earlier proposed that the point of union would be posterior to the velum chamber such that feeding and breathing would not conflict. However, Holmes et al. (2011) published an image of a species which they tentatively identified as *E. stoutii* that appears to contradict this conclusion.

Using CT (Fig. 6B), MRI (Fig. 6C–E) and dissection (Fig. 6F,G) images of the anterior hagfish body, and visual observation of velar movement (Movie 2), we rejected the more anterior location of the velum chamber suggested earlier (Eom and Wood, 2019), and accepted the more posterior location of the velum chamber labelled by Holmes et al. (2011) in their published magnetic resonance image. This means that the oronasal septum, which separates the water flow pathway from the food pathway, terminates at the anterior end, rather than the posterior end of the velum chamber (Fig. 6F–H). Our earlier conclusion had been supported by measurements of reciprocal pressure changes in the nostril and mouth cavity of non-feeding animals, a point to be discussed below.

How do hagfish transfer the engulfed large prey objects from mouth to intestine, and integrate this with breathing?

With the new interpretation as to the location of the velum chamber, prey objects hooked into the mouth cavity by the horny dental teeth and the contraction of the medio-rostral part of the basal plates (Fig. 5) would be transferred into the velum chamber, rather than behind it. When the hagfish is not feeding, the cyclic velum chamber contractions generate suction for continuous unidirectional inflow of water through the nostril, and positive pressure forcing water down the long pharynx (Eom and Wood, 2019). Considering the size of the prey chunks (up to 10% of body mass), the prey objects would block this major respiratory pump such that the nostril ventilation and water flow down the pharynx would be transiently disabled.

However, the hagfish can still exhale water stored in the gill pouches by gill pouch contraction, creating a vacuum in the respiratory tract, because the decreased pressure from the gill pouches cannot be relieved by water inhalation through the nostril duct at this time. This vacuum would help to quickly move the food item past the velum chamber. Additionally, the hagfish frequently showed ventral muscle contraction (Fig. 1D; Movie 1) when they extruded their dental plates (Fig. 1A–C). After engulfment, the hagfish vigorously shook their anterior body in an undulatory, peristaltic fashion in association with very clear ventral muscle contraction. The prey objects were quickly transferred to the intestine (within 5 s) across the ∼10 cm length of pharynx (Movie 1). This repeated peristaltic contraction moved from the anterior to the posterior gill pouches, and lasted until the hagfish successfully transferred the engulfed prey objects into the intestine (Fig. 1D). The ventral muscle contraction stopped as soon as the hagfish resumed a coiled posture. We conclude that hagfish use the nostril and mouth alternately, and that the interruption of breathing is short lasting. In this regard, it is relevant that non-feeding hagfish routinely exhibit periods of complete apnoea (Eom and Wood, 2019), and can stop breathing for prolonged periods when exposed to noxious ammonia (Eom et al., 2019). In future, measurements of pressure in various parts of the system and of nostril flow during the actual feeding event will be needed to substantiate these ideas, and unfortunately will be very difficult to obtain.

Another point needing further exploration is that our earlier measurements in non-feeding hagfish clearly showed pressure peaks in the mouth coinciding with negative pressure troughs and flow peaks in the nostril (Eom and Wood, 2019). Thus, even though the two pathways are not separate but rather meet at the entrance of the velum chamber, they appear to be kept functionally separate. Perhaps the posterior end of the oronasal septum acts as a uvula-type flap, alternately closing off one or the other pathway, an idea to be tested in future experiments.

Different oxygen utilization in different gill pouches

Our second hypothesis was that there would be a morphological basis for the increasing gradient in O_2 utilization from the anterior to posterior gill pouches seen in resting fasted hagfish (Fig. 4A). Earlier, we had suggested that one possibility would be sequential direct passage of some respired water from anterior to posterior gill pouches (Eom and Wood, 2021). However, based on the anatomical results shown in Fig. 7, we are now confident that there are no direct water connections from one gill pouch to the next, so another explanation is needed. Partial rebreathing of water by backflow from anterior pouches into the pharynx remains a possibility, as does O_2 uptake by the pharyngeal wall itself (Eom and Wood, 2021). However, the present findings on vascular anatomy provide another

possible explanation – the different anatomy of the ventral aorta serving anterior versus posterior gill pouches. The anterior ventral aorta is bifurcated into parallel, progressively narrowing branches supplying blood to the 5th to 1st gill pouches (Fig. 7D), but the posterior ventral aorta is a single larger vessel directly connecting the heart to the 12th to 6th gill pouches (Fig. 7E). As a result of bifurcation, the cross-sectional area of the anterior ventral aorta is much smaller than that of the posterior ventral aorta. Thus, we propose that as we move anteriorly, the gill pouches receive progressively less blood flow, and therefore are less effective in O_2 extraction from the water (Fig. 4A). Further studies are required to understand the benefit of ventral aorta bifurcation and lower O_2 utilization in the anterior gill pouches in resting, non-fed hagfish, and how this is overcome after feeding in hagfish (Fig. 4B).

The contributions of O_2 utilization, $\dot{V}_w$, SV_w and f_R to increased $\dot{M}_{O_2}$ after feeding

Our third hypothesis was that increased $\dot{M}_{O_2}$ after feeding would be accompanied by little change in O_2 utilization, but rather by increases in $\dot{V}_w$ due to elevations in both SV_w and f_R. In the first hour after feeding, when $\dot{M}_{O_2}$ was already significantly elevated by 2.5-fold (Fig. 3E), this hypothesis was clearly not supported because $\dot{V}_w$ did not change significantly (Fig. 3B) despite an increase in SV_w (Fig. 3A), whereas O_2 utilization almost doubled (Figs 3D, 4). However, at 24 h after feeding, $\dot{M}_{O_2}$ was still elevated, but utilization had returned to control values (Fig. 3D), and now increased SV_w (Fig. 3B), driven by increased f_R (Fig. 3A), was the major contributor. Clearly, the situation is more complex than seen previously with spontaneous hyperventilation (Eom and Wood, 2021), on which the hypothesis was based, and the hagfish has several options at its disposal for increasing $\dot{M}_{O_2}$. In the first hour, the strategy of high O_2 extraction efficiency, and unchanged flow, as a result of increased SV_w but reduced f_R, may represent a more efficient mechanism. This increased O_2 utilization (66%) after feeding brings the low utilization (35%) of the resting hagfish into the range (55–80%) reported for resting teleosts with similar benthic lifestyles (Eddy, 1974; Lomholt and Johansen, 1979; Wood et al., 1979). Possible explanations include increased blood flow to the gill pouches, increased diffusive conductance, and/or decreased venous O_2 levels. However, there are no measurements of these parameters in post-feeding hagfish, or to our knowledge even in post-feeding teleosts, so this is an important topic for future investigation. At later times, elevations in $\dot{M}_{O_2}$ became more dependent upon elevation of flow due to increased f_R.

One important caveat with respect to the results of Fig. 3 is that there was only a single pre-feeding control point, and no simultaneous control group measurements at the same times (1, 4, 24 h) as for the fed hagfish. It is possible that some of the same changes in respiratory parameters could have occurred in non-fed animals at these times. However, this concern is somewhat alleviated by the observation that there were no significant variations in these parameters in the non-fed control hagfish at these same times in series II (Fig. 2).

Magnitude of the increase in $\dot{M}_{O_2}$ after feeding

Our results are supportive but not unequivocal with respect to our fourth hypothesis. We had predicted that the large ration (~ 20% of body mass) associated with engulfment feeding would result in more marked elevation of $\dot{M}_{O_2}$ than reported in two previous studies. These investigations, one on *E. stoutii* (Weinrauch et al., 2018) using natural feeding by carcass burrowing (ration unknown), the other on *Eptatretus cirrhatus* (Glover et al., 2019) using gavage feeding (5% ration), reported comparable relative increases in $\dot{M}_{O_2}$ after feeding, peaking at 1.9- to 3-fold, but with different time courses, with maxima at 8 h in the former and 24 h in the latter. Comparison of our results with those of Weinrauch et al. (2018) is particularly relevant, as the two studies were performed at the same temperature, on the same species collected from the same location, but with different feeding protocols. Our series II experiment (Fig. 2) provides the fairer comparison, as the fish were not instrumented and the measurements were made by closed system respirometry in both investigations. In our experiments, the elevation in $\dot{M}_{O_2}$ was very rapid (within 1 h) and remained significant to 12 h (Fig. 2), perhaps reflecting the very large meals ingested. Weinrauch et al. (2018) made their first measurement at 4 h, where there was no increase, and detected a significant increase only at 8 h; subsequent $\dot{M}_{O_2}$ measurements were slightly elevated at 12–36 h, but none of these values were significantly different from their pre-feeding control value. Another difference was in absolute $\dot{M}_{O_2}$ values; our measurements (Fig. 2) under both control and post-feeding conditions were about 50% lower than those of Weinrauch et al. (2018). However, in our series III, where the fish were instrumented and therefore disturbance was greater, both control and post-feeding peak $\dot{M}_{O_2}$ values were similar to those reported by Weinrauch et al. (2018), but our $\dot{M}_{O_2}$ elevation remained significant at 24 h (Fig. 3E). Overall, these results suggest that had we extended our measurements to a longer time course, even larger cumulative increases in $\dot{M}_{O_2}$ might have been recorded, especially in light of the slow time course of digestion.

The post-prandial elevations in $\dot{M}_{O_2}$ reflect specific dynamic action (SDA), the metabolic cost of processing the meal – digestion, absorption, metabolic interconversions and protein synthesis (Secor, 2009). Note that in series II, typical 'pre-feeding activity' was induced in the non-fed controls by exposure to anchovy juice, yet immediate post-feeding elevations in $\dot{M}_{O_2}$ were still significantly greater in the experimental animals that were also exposed to the juice and allowed to ingest the anchovy chunks (Fig. 2). This eliminates excitement as a major cause of the increased metabolic rate. There was however a tendency (non-significant) for $\dot{M}_{O_2}$ to rise over time in the controls, peaking at the same time (12 h) as the highest values in the animals that fed (Fig. 2). Possible explanations include a diurnal variation in metabolic rate and/or initial absorption of some nutrients from the anchovy juice through the body surface (Glover et al., 2011), eliciting a minor SDA response in the controls.

Slow digestion process in hagfish

Based on the appearance of faecal material, the hagfish completely digested the soft tissue of engulfed prey objects equivalent to ~20% of body mass within 2 days and excreted the used gut membrane in 5 days. During this whole period, the fed hagfish maintained a coiled posture and up to 48 h barely responded to any physical contact such as pinching by forceps or transferring from tank to tank. Known defence behaviours, such as knotting behaviour and slime generation, were also suppressed. However, overall responsiveness to disturbance was dramatically increased after the hagfish excreted bony structures and scales within 2 days post-feeding, thereafter showing similar responsiveness to non-fed hagfish between 2 and 5 days.

After finishing the digestion process, the hagfish excreted the used gut membrane (Fig. 1H–J), known as the peritrophic membrane (Adam, 1966). Comparable specialized chitin-based mesh membrane structures are commonly observed in the guts of

invertebrates, but occur in few vertebrates (Engel and Moran, 2013; Nakashima et al., 2018). The major functions of the peritrophic membrane in invertebrates have been summarized by Glover and Weinrauch (2019), and include promoting digestion, serving as a structural barrier to protect the gut epithelium and segregating the gut microbiome from the epithelium. Further studies are required to understand the functional roles of the peritrophic membrane in the hagfish digestive process, and especially the nature of the hagfish intestinal microbiome.

Future directions

In a recent review of the feeding physiology of hagfish, Glover and Weinrauch (2019) highlighted the need for far more work in this field on an important group close to the base of vertebrate evolution. However, they noted that: 'Many of the key tools of the experimental biologist are compromised by a species that does not readily feed in captivity, is difficult to instrument, and which produces copious quantities of slime'. In the present study, we have been able to overcome some of these impediments by using simple approaches such as very gentle handling, careful instrumentation, and experimentation during the hours of darkness in diffuse light, thereby producing valuable new knowledge. This knowledge has been supplemented by respirometry and both classical and state-of-the art morphological techniques. Future studies should employ comparable methodologies to examine the feeding versus breathing interface over a longer post-prandial period, with different meal sizes, under different O_2 regimes and on hagfish species with different trophic habits. Ideally, the present methodology should be ultimately improved such that physiological changes during the actual feeding event can be recorded.

Acknowledgements

We thank Drs Tony Farrell, Colin Brauner and Bill Milsom for the loan of equipment, BMSC Research Coordinators Dr Eric Clelland and Tao Eastham for invaluable support, and two anonymous reviewers whose constructive comments improved the manuscript.

Competing interests

The authors declare no competing or financial interests.

Author contributions

Conceptualization: J.E., C.M.W.; Methodology: J.E., H.L., C.M.W.; Software: J.E., H.L.; Validation: J.E., H.L., C.M.W.; Formal analysis: J.E.; Investigation: C.M.W.; Resources: C.M.W.; Data curation: J.E.; Writing - original draft: J.E.; Visualization: J.E., H.L.; Supervision: C.M.W.; Project administration: C.M.W.; Funding acquisition: C.M.W.

Funding

This work was supported by a Natural Sciences and Engineering Research Council of Canada (NSERC) Discovery grant (RGPIN-2017–03843), with additional covid relief funding, to C.M.W.

References

Adam, H. (1966). Peritrophic membranes in the intestine of the hagfish *Myxine glutinosa*. In *Phylogeny of Immunity* (ed. R. T. Smith, P. A. Miescher and R. A. Good), pp. 147. University of Florida Press.

Bardack, D. (1998). Relationships of living and fossil hagfishes. In *Biology of Hagfishes* (ed. J. M. Jørgensen, J. P. Lomholt, R. E. Weber and H. Malte), pp. 3-14. New York: Springer.

Bartels, H. (1998). The gills of hagfishes. In *Biology of Hagfishes* (ed. J. M. Jørgensen, J. P. Lomholt, R. E. Weber and H. Malte), pp. 205-222. New York: Springer.

Boutilier, R. G., Heming, T. A. and Iwama, G. K. (1984). Appendix: Physicochemical parameters for use in fish respiratory physiology. In *Fish Physiology* (ed. W. S. Hoar and D. J. Randall), pp. 403-430. New York: Elsevier.

Braun, C. B. and Northcutt, G. R. (1998). Cutaneous exteroreceptors and their innervation in hagfishes. In *Biology of Hagfishes* (ed. J. M. Jørgensen J. P. Lomholt R. E. Weber and H. Malte), pp. 512-532. New York: Springer.

Clark, A. J. and Summers, A. P. (2007). Morphology and kinematics of feeding in hagfish: possible functional advantages of jaws. *J. Exp. Biol.* **210**, 3897-3909. doi:10.1242/jeb.006940

Clark, A. J., Maravilla, E. J. and Summers, A. P. (2010). A soft origin for a forceful bite: motor patterns of the feeding musculature in Atlantic hagfish, *Myxine glutinosa*. *Zoology (Jena)* **113**, 259-268. doi:10.1016/j.zool.2010.02.001

Eddy, F. B. (1974). Blood gases of the tench (*Tinca tinca*) in well aerated and oxygen-deficient waters. *J. Exp. Biol.* **60**, 71-83. doi:10.1242/jeb.60.1.71

Ellis, J. E., Rowe, S. and Lotze, H. K. (2015). Expansion of hagfish fisheries in Atlantic Canada and worldwide. *Fisher. Res.* **16**, 24-33. doi:10.1016/j.fishres.2014.06.011

Engel, P. and Moran, N. A. (2013). The gut microbiota of insects – diversity in structure and function. *FEMS Microbiol. Rev.* **37**, 699-735. doi:10.1111/1574-6976.12025

Eom, J. and Wood, C. M. (2019). The ventilation mechanism of the Pacific hagfish *Eptatretus stoutii*. *J. Fish Biol.* **94**, 261-276.

Eom, J. and Wood, C. M. (2021). Understanding ventilation and oxygen uptake of Pacific hagfish (*Eptatretus stoutii*), with particular emphasis on responses to ammonia and interactions with other respiratory gases. *J. Comp. Physiol. B.* **191**, 255-271. doi:10.1007/s00360-020-01329-7

Eom, J., Giacomin, M., Clifford, A. M., Goss, G. G. and Wood, C. M. (2019). Ventilatory sensitivity to ammonia in the Pacific hagfish (*Eptatretus stoutii*), a representative of the oldest extant connection to the ancestral vertebrates. *J. Exp. Biol.* **222**, jeb199794. doi:10.1242/jeb.199794

Glover, N. C. and Bucking, C. (2015). Feeding, digestion, and nutrient absorption in hagfish. In *Hagfish Biology* (ed. D. H. Evans and S. Bortone), pp. 299-320. Boca Raton: CRC Press.

Glover, C. N., Bucking, C. and Wood, C. M. (2011). Adaptations to in situ feeding: novel nutrient acquisition pathways in an ancient vertebrate. *Proc. R. Soc. B* **278**, 3096-3101. doi:10.1098/rspb.2010.2784

Glover, N. C. and Weinrauch, A. M. (2019). The good, the bad and the slimy: experimental studies of hagfish digestive and nutritional physiology. *J. Exp. Biol.* **222**, jeb190470. doi:10.1242/jeb.190470

Glover, C. N., Weinrauch, A. M., Bynevelt, S. and Bucking, C. (2019). Feeding in *Eptatretus cirrhatus:* effects on metabolism, gut structure and digestive processes, and the influence of post-prandial dissolved oxygen availability. *Comp. Biochem. Physiol. A.* **229**, 52-59. doi:10.1016/j.cbpa.2018.11.023

Holmes, W. M., Cotton, R., Xuan, V. B., Rygg, A. D., Craven, B. A., Abel, R. L., Jonathan, R. S. and Cox, P. L. (2011). Three-dimensional structure of the nasal passageway of a hagfish and its implications for olfaction. *Anat. Rec.* **294**, 1045-1056. doi:10.1002/ar.21382

Johansen, K. and Strahan, R. (1963). The respiratory system of *Myxine glutinosa* L. In *The Biology of Myxine* (ed. A. Bordal and R. Fänge), pp. 352-371. Oslo: Universitetsforlaget.

Li, S. and Wang, F. (2021). Vertebrate evolution conserves hindbrain circuits despite diverse feeding and breathing modes. *eNeuro* **8**, ENEURO 0435-20.2021. doi:10.1523/ENEURO.0435-20.2021

Lomholt, J. P. and Johansen, K. (1979). Hypoxia acclimation in carp – how it affects O_2 uptake, ventilation and O_2 extraction from water. *Physiol. Zool.* **52**, 38-49. doi:10.1086/physzool.52.1.30159930

Mallatt, J. and Paulsen, C. (1986). Gill ultrastructure of the Pacific hagfish *Eptatretus stoutii*. *Am. J. Anat.* **177**, 243-269. doi:10.1002/aja.1001770209

Malte, H. and Lomholt, J. P. (1998). Ventilation and gas exchange. In *Biology of hagfishes* (ed. J. M. Jørgensen, J. P. Lomholt, R. E. Weber and H. Malte), pp. 223-234. New York: Springer.

Martini, F. H. (1998). The ecology of hagfishes. In *Biology of hagfishes* (ed. J. M. Jørgensen, J. P. Lomholt, R. E. Weber and H. Malte), pp. 57-77. New York: Springer.

Miyashita, T. (2020). A Paleozoic stem hagfish Myxinikela siroka – revised anatomy and implications for evolution of the living jawless vertebrate lineages. *Can. J. Zool.* **98**, 850-865. doi:10.1139/cjz-2020-0046

Nakashima, K., Kimura, S., Ogawa, Y., Watanabe, S., Soma, S., Kaneko, T., Yamada, L., Sawada, H., Tung, C. H., Lu, T. M. et al. (2018). Chitin-based barrier immunity and its loss predated mucus-colonization by indigenous gut microbiota. *Nat. Commun.* **9**, 1-13. doi:10.1038/s41467-017-02088-w

Oisi, Y., Ota, K. G., Fujimoto, S., Kuratani, S. (2013). Development of the chondrocranium in Hagfishes, with special reference to the early evolution of vertebrates. *Zool. Sci.* **30**, 944-961. doi:10.2108/zsj.30.944

Perry, S. F., Vulesevic, B., Braun, M. H. and Gilmour, K. (2009). Ventilation in Pacific hagfish (*Eptatretus stoutii*) during exposure to acute hypoxia or hypercapnia. *Resp. Physiol. Neurobiol.* **167**, 227-234. doi:10.1016/j.resp.2009.04.025

Secor, S. M. (2009). Specific dynamic action: a review of the postprandial metabolic response. *J. Comp. Physiol. Biochem. B.* **179**, 1-56. doi:10.1007/s00360-008-0283-7

Shelton, R. G. J. (1978). On the feeding of the hagfish *Myxine glutinosa* in the North Sea. *J. Mar. Biol. Assoc.* **58**, 81-86. doi:10.1017/S0025315400024413

Strahan, R. (1958). The velum and respiratory current of *Myxinej*. *Acta Zool.* **39**, 227-240.

Tamburri, M. N. and Barry, J. P. (1999). Adaptations for scavenging by three diverse bathyal species, *Eptatretus stoutii, Neptunea amianta* and *Orchomene obtusus*. *Deep-Sea Res.* **46**, 2079-2093. doi:10.1016/S0967-0637(99)00044-8

Theisen, B. (1973). The olfactory system in the hagfish *Myxine glutinosa*. I. Fine structure of the apical part of the olfactory epithelium. *Acta Zool.* **54**, 271-284.

Weinrauch, A. M., Clifford, A. M. and Goss, G. G. (2018). Post-prandial physiology and intestinal morphology of the Pacific hagfish (*Eptatretus stoutii*). *J. Comp. Physiol. B.* **188**, 101-112. doi:10.1007/s00360-017-1118-1

Wilkie, M. P., Clifford, A. M., Edwards, S. L. and Goss, G. G. (2017). Wide scope for ammonia and urea excretion in foraging Pacific hagfish. *Mar. Biol.* **164**, 126. doi:10.1007/s00227-017-3148-3

Wood, C. M., McMahon, B. R. and McDonald, D. G. (1979). Respiratory gas exchange in the resting starry flounder, *Platichthys stellatus*: a comparison with other teleosts. *J. Exp. Biol.* **78**, 167-179. doi:10.1242/jeb.78.1.167

Zintzen, V., Roberts, C. D., Anderson, M. J., Stewart, A. L., Struthers, C. D. and Harvey, E. S. (2011). Hagfish predatory behaviour and slime defence mechanism. *Sci. Rep.* **1**, 131. doi:10.1038/srep00131